British Journal of Pharmacology (2009), 156, 48–61

0007-1188/08
www.brjpharmacol.org

RESEARCH PAPER

A standardized extract of *Ginkgo biloba* suppresses doxorubicin-induced oxidative stress and p53-mediated mitochondrial apoptosis in rat testes

Y-C Yeh[1], T-J Liu[1,2], L-C Wang[1], H-W Lee[1], C-T Ting[1,2], W-L Lee[1,2], C-J Hung[1], K-Y Wang[1,3], H-C Lai[4] and H-C Lai[1,2]

[1]*Cardiovascular Center, Taichung Veterans General Hospital, Taichung, Taiwan,* [2]*Departments of Medicine, Surgery, and Cardiovascular Research Center, National Yang-Ming University School of Medicine, Taipei, Taiwan,* [3]*Department of Medicine, Chuan-Shan Medical University, Taichung, Taiwan, and* [4]*Chang-Gung University College of Medicine, Tao-Yuan and Chang-Gung Memorial Hospital, Lin-Koh Taipei, Taiwan*

Background and purpose: Doxorubicin evokes oxidative stress and precipitates cell apoptosis in testicular tissues. The aim of this study was to investigate whether the *Ginkgo biloba* extract 761 (EGb), a widely used herbal medicine with potent anti-oxidant and anti-apoptotic properties, could protect testes from such doxorubicin injury.
Experimental approach: Sprague-Dawley male rats (8 weeks old) were given vehicle, doxorubicin alone (3 mg kg^{-1} every 2 days for three doses), EGb alone (5 mg kg^{-1} every 2 days for three doses), or EGb followed by doxorubicin (each dose administered 1 day after EGb). At 7 days after the first drug treatment oxidative and apoptotic testicular toxicity was evaluated by biochemical, histological and flow cytometric analyses.
Key results: Compared with controls, testes from doxorubicin-treated rats displayed impaired spermatogenesis, depleted haploid germ cell subpopulations, increased lipid peroxidation products (malondialdehyde), depressed antioxidant enzyme activities (superoxide dismutase, glutathione peroxidase and glutathione), reduced antioxidant enzyme expression (superoxide dismutase) and elevated apoptotic indexes (pro-apoptotic modulation of Bcl-2 family proteins, intensification of p53 and Apaf-1, release of mitochondrial cytochrome *c*, activation of caspase-3 and increase of terminal deoxynucleotidyl transferase nick-end labelling/sub-haploid cells), while EGb pretreatment effectively alleviated all of these doxorubicin-induced abnormalities in testes.
Conclusions and implications: These results demonstrate that EGb protected against the oxidative and apoptotic actions of doxorubicin on testes. EGb may be a promising adjuvant therapy medicine, potentially ameliorating testicular toxicity of this anti-neoplastic agent in clinical practice.
British Journal of Pharmacology (2009) **156**, 48–61; doi:10.1111/j.1476-5381.2008.00042.x

Keywords: EGb; doxorubicin; testis; apoptosis; oxidative stress; cytochrome c; p53

Abbreviations: DAPI, 4′,6′ diamidino-2-phenylindole; Dox, doxorubicin; EGb, *Ginkgo biloba* extract 761; GPx, glutathione peroxidase; MDA, malondialdehyde; SOD1, Cu/Zn superoxide dismutase; SOD2, Mn superoxide dismutase; TUNEL, terminal deoxynucleotidyl transferase nick-end labelling

Introduction

Doxorubicin (Dox) has been widely employed for treatment of various haematological and solid tumours in the past four decades. Its application, however, carries the risk of serious dose-dependent toxicity to other non-target tissues (Tan *et al.*, 1973). The testis is among the non-target tissues that are vulnerable to side effects of this potent chemotherapeutic agent (Da Cunha *et al.*, 1983; Suter *et al.*, 1997), in which Dox could strikingly impede spermatogenesis (Howell and Shalet, 2005; Yeh *et al.*, 2007) and lead eventually to infertility. The mechanism responsible for this testicular toxicity of Dox is not yet completely clear, but findings from recent studies strongly suggest oxidative stress from lipid peroxidation (Atessahin *et al.*, 2006; Yeh *et al.*, 2007) and cellular apoptosis (Shinoda *et al.*, 1999) as being major causes. Based on this

Correspondence: H-C Lai, Taichung Veterans General Hospital, 160, Sec 3, Taichungkang Rd, Taichung, 407, Taiwan. E-mail: tsunjuiliu@gmail.com
Y-C Yeh and T-J Liu contributed equally to this paper.
Received 10 March 2008; revised 12 August 2008; accepted 19 September 2008

concept, a variety of anti-oxidant or anti-apoptotic agents have been employed to counteract Dox-induced testicular damage (Jahnukainen *et al*., 2001; Hou *et al*., 2005). Nevertheless, so far there is still no single agent proven effective enough to prevent or reverse this adverse effect.

Leaves of the plant *Ginkgo biloba* have been used for thousands of years as a traditional Chinese herbal medicine (Logani *et al*., 2000). Recently, a standardized chemical product from these leaves was pharmacologically prepared containing two major functional constituents (24–25% flavonoid glycosides and 6% terpenoids) (Shen *et al*., 1998). This standardized extract, or *Ginkgo biloba* extract 761,(EGb), is widely utilized for treatment of several nervous system diseases (Lu *et al*., 2006) for its anti-oxidant and anti-platelet properties (Gohil, 2002; DeFeudis *et al*., 2003). Furthermore, this extract has been shown to modulate expression of apoptotic related genes, reduce generation of free radicals and increase activity of antioxidant enzymes in various types of animal tissues and cells (Timioglu *et al*., 1999; Logani *et al*., 2000; DeFeudis *et al*., 2003), implying it to be a promising cytoprotective agent aginst a range of exogenous toxic stimuli. To determine whether EGb could also attenuate Dox-induced apoptosis and oxidative stress in testicular tissue, this study was designed to examine the antagonistic actions of EGb on pathological and molecular biological abnormalities in rat testes, induced by Dox. The results of this study could clarify the role of the popular herbal drug EGb in prevention of Dox testicular injury, and may shed light on the ultimate solution to this very serious testicular side effect of Dox treatment.

Methods

Experimental animals and pharmacological treatments
All animal procedures and the experimental protocols were approved by the Institutional Animal Care and Use Committee at Taichung Veterans Hospital and were carried out in accordance with the *Guide for the Care and Use of Laboratory Animals*. Male Sprague-Dawley rats weighing 210 to 225 (5–6 weeks of age) were obtained from the National Animal Center, housed under controlled conditioning (25 ± 1°C constant temperature, 55% relative humidity, 12 h lighting cycle), and received standard pelleted diet and water *ad libitum* during the study period. Forty rats at 8 weeks old, equivalent to humans at the age of young adulthood (Quinn, 2005), were randomly assigned to four groups as described below according to the pharmacological treatment they received. The control group (Cont) of rats received only normal saline injection. The Dox group (Dox) rats were given Dox (3 mg kg^{-1}; i.p.) every 2 days for a total of three injections, equal to an accumulated dose of 9 mg kg^{-1} (Jahnukainen *et al*., 2001). The EGb group (EGb) of rats received EGb (5 mg kg^{-1}; i.p.) every 2 days for a total of three times and equivalent to an accumulated dose of 15 mg kg^{-1} (DeFeudis *et al*., 2003). The EGb-Dox group (EGbDox) of rats uwere given the same dose of EGb as the EGb group, followed by an identical dose of Dox, to the Dox group (each dose given 1 day after EGb).

Collection of serum and testicular samples
Rats were killed on day 7 after the first treatment. The body and testicular weights of all animals were measured and compared with their baseline values and between groups. Blood samples were drawn from the caudal vena cava, collected in test tubes containing EDTA, and centrifuged at 1500× *g* for 10 min to obtain serum for evaluating the expression of superoxide dismutase (SOD) proteins. The testicular tissues were either fixed in 10% formalin for histopathologic examinations and 4% paraformaldehyde for immunofluorescent microscopy, or stored at –80°C in association with the serum samples till later analysis, unless otherwise mentioned for specific examinations.

Epididymal sperm counts
The spermatozoa were collected and examined from the caudal epididymis of each testicular sample, as previously reported (Atessahin *et al*., 2006). Briefly, the epididymal cauda was cut into small pieces in a 35 mm Petri dish and placed in a centrifuge tube containing 3 mL of normal saline to let the sperms swim up for 10 min at 37°C. After dilution with Trypan blue solution (. . .), the specimen was transferred to the counting chamber of the haemacytometer and was allowed to stand for 5 min. The cells were then counted under an inverted microscope (Leica, DMIL, Bensheim, Germany). The total epididymal sperm numbers obtained from the counting were expressed as the number of sperms per testis ($\times 10^6$).

Spermatogenic structural changes in the seminiferous tubules
Testicular tissues for histopathological examination were fixed in 10% buffered formalin overnight and then embedded with paraffin. When analyzed, all paraffin-embedded tissue was sectioned at 5 μm, deparaffinized in xylene, dehydrated by ethyl alcohol in decreasing concentrations (100%, 95% and 70%), and stained with haematoxylin (Merck KGaA, Darmstadt, Germany) and eosin (Sigma, St. Louis, MO, USA). These specimens were examined under bright-field optical microscopy using a light microscope (Leica, DMR, Bensheim, Germany), and corresponding digital images were captured for later analysis by a Spot CCD Camera driven by Advanced Spot RT Software version 3.3 (Diagnostic Instruments Inc., MI, USA). The total number and the mean diameter of the seminiferous tubules in 10 random microscopic fields of each testicular section were then measured under the microscope at 100× magnification. At least six sections of testicular tissue from each rat were examined and the averages of these values taken for the number and the diameter of the seminiferous tubules of this group of animals.

Oxidative stress in testicular tissues and in the circulation
Oxidative status in testicular tissues could be estimated from the concentrations of malondialdehyde (MDA), a direct indicator of reactive oxygen species-induced lipid peroxidation (Timioglu *et al*., 1999; Atessahin *et al*., 2006), and glutathione (GSH), also an important indicator of oxidative stress. We also used the activity of two representative antioxidant enzymes,

SOD and glutathione peroxidase (GPx) (Bauche *et al*., 1994; Sikka, 2004). To measure these indicators, fresh testicular tissues were homogenized in a lysis buffer (0.25 M sucrose, 10 mmol·L^{-1} Tris-HCl and 1 mmol·L^{-1} EDTA adjusted to pH 7.4) and centrifugated at 10 000× *g* for 20 min. The supernatants were collected and the protein concentrations were determined using Bradford Protein Assay (Bio-Rad Laboratories, Hercules, CA, USA) (Bradford, 1976). The assay for MDA was then carried out with the fluorometric method described earlier (Koksal *et al*., 2002), which detected the reaction of the sample with thiobarbituric acid to quantitate the resultant lipid peroxidation as a surrogate of MDA level. Total GSH levels were determined by the glutathione disulphide reductase-5,5′ dithiobis-(2-nitrobenzoic acid) recycling assay using the Glutathione Assay Kit (BioChain, CA, USA), which estimated the content of tissue GSH from the standard curve simultaneously obtained under the same conditions with standard solution. Total SOD activity in homogenized testicular tissues was estimated from the ability of the tissue to inhibit cytochrome *c* reduction in a xanthine-xanthine oxidase generation system (RANSOD, RANDOX Laboratories Ltd., Antrim, UK) (Mohan *et al*., 2006). The GPx activity was determined spectrophotometrically using a commercially available kit (RANSEL, RANDOX Laboratories Ltd., Antrim, UK), which estimated the amount of tissue GPx from the reduction of cumene hydroperoxide and oxidation of NADPH to $NADP^+$, as reflected by the decrease in absorbance at 340 nm (Bauche *et al*., 1994).

The amounts of Cu/Zn superoxide dismutase (SOD1) and Mn superoxide dismutase (SOD2) in the circulation were measured by enzyme-linked immunosorbent assay (ELISA). Briefly, 96-well polyvinyl plates (Immulon II, Dynatech Labs, Chantilly, VA, USA) were coated with 10 ng of whole serum in 10 mmol·L^{-1} sodium carbonate at pH 9.6 and left overnight at 4°C. Plates were subsequently incubated with 3% bovine serum alb (BSA) for 30 min at room temperature to block non-specific binding. Dilutions of rabbit anti-SOD1 and goat anti-SOD2 antibodies ranging from 1:100 to 1:10^8 were added and left at room temperature for 1 h. Horseradish peroxidase (HRP)-conjugated goat anti-rabbit or rabbit anti-goat IgG was then added to react for 1 h. Plates were finally washed extensively and the chromogen *o*-phenylenediamine (Sigma, St. Louis, MO, USA) was added to demonstrate activity. Plates were read with an ELISA reader (MrX, Dynatech Lab.) at a wavelength of 490 nm. Quantitative expressions of SOD1 and SOD2 were acquired from conversion of the optical density (OD) based on the standard calibration curve simultaneously obtained under the same conditions from standard solutions of SOD1 and SOD2 (Sigma). Results were averaged from triplicate extracts of each specimen and expressed by their means.

Immunoblotting

For immunoblotting analysis of the impact of Dox and EGb on apoptosis-related signalling effectors, testicular tissues were lysed with a lysis buffer [50 mmol·L^{-1} Tris-HCl pH 7.5; 150 mmol·L^{-1} KCl; 5 mmol·L^{-1} $MgCl_2$, 0.25 mol·L^{-1} sucrose, 0.1 mmol·L^{-1} dithiothreitol (DTT), 1 mmol·L^{-1} PMSF; 2 μg mL^{-1} leupeptin, 2 μg mL^{-1} pepstain A and 1% NP-40] and were centrifuged at 10 000× *g* at 4°C for 20 min to obtain the cellular proteins in the supernatant. The protein concentrations were determined, and equal amount of proteins from each sample was resolved by SDS-PAGE, transferred to polyvinylidene difluoride membranes and blocked in blocking buffer (150 mmol·L^{-1} NaCl in 10 mmol·L^{-1} Tris, pH 7.5 containing 5% non-fat dry milk) for 1 h at room temperature. The membranes were incubated with primary antibodies overnight at 4°C, washed three times (20 mmol·L^{-1} Tris-HCl, pH 7.5, 137 mmol·L^{-1} NaCl and 0.1% Tween 20), incubated with HRP-conjugated secondary antibodies (1:5000 dilution) for 1 h at room temperature, washed three times and detected with ECL (Pierce Chemical Co., Rockford, IL, USA). The density of each protein band was determined using Sciencelab ImageGauge 4.0 Software (Fuijifilm, Tokyo, Japan) and compared by densitometry.

Immunofluorescence microscopy

Freshly dissected testes were fixed in 4% paraformaldehyde and embedded in OCT compound (Sakura Finetek, Torrance, CA, USA). Cryosections (10 μm thick) were mounted on glass slides, washed in phosphate buffered saline (PBS) and immersed in 3% BSA for 1 h to block nonspecific binding. These slides were then incubated with primary mouse antibodies against SOD1, Bcl-2 or Bax at dilutions of 1:100 for 18 h at 4°C, washed twice in PBS/Tween-20 solution, incubated with a fluorescein- or Texas Red-conjugated secondary antibodies for 1 h at room temperature and photographed with a laser scanning confocal microscope (Leica, TCSNT, Bensheim, Germany). Certain sections were incubated with 4′,6′ diamidino-2-phenylindole (DAPI; Sigma, St. Louis, MO, USA) containing mounting medium for nuclear counterstaining.

In situ detection of apoptosis

Apoptosis of testicular cells was identified by terminal deoxynucleotidyl transferase nick-end labelling (TUNEL) assay using the In Situ Cell Death Detection Kit, Fluorescein (Roche, Ltd, Basel, Switzerland). Paraffin-embedded sections of testicular tissue (5 μm) from five rats of each group were deparaffinized in xylene and dehydrated in a graded ethanol series (100%, 95% and 70%) as above. The slides were incubated with proteinase K (20 μg mL^{-1}) at room temperature for 15 min and then washed with PBS solution. Specimens were then treated with equilibrium buffer for 10 min and incubated with a terminal deoxynucleotidyl transferase (TdT) reaction mixture for 1 h at 37°C in a humidified chamber to catalyze the addition of fluorescein-dUTP labels to free 3′-OH groups at single- and double-stranded DNA breaks. At least three sections from each specimen were then counterstained with DAPI (Sigma, St. Louis, MO, USA) after washing twice with PBS solution. The label incorporated at the damaged sites of the DNA, indicating apoptosis, was visualized and photographed by confocal laser scanning microscopy (Leica, TCSNT, Bensheim, Germany). Digital images from 10 random microscopic fields of each section were captured and imported into Adobe Photoshop 7.0 (Adobe System Inc.). The ratio of total TUNEL-positive cells to total DAPI-stained cells represented the apoptotic index of the sample and was compared between groups.

Flow cytometric measurements of testicular cell populations
Flow cytometry is a powerful tool for differentiating spermatogenetic cells at specific division stages (Malkov *et al.*, 1998) and evaluating alterations of predominant testicular cell populations after drug administration (Yoon *et al.*, 2003). To assess the disruption by Dox and the protective effect of EGb on spermatogenesis, testicular cells were prepared as reported elsewhere (Suter *et al.*, 1997; Malkov *et al.*, 1998). In short, testes were excised, decapsulated, cut into small pieces, transferred to a 100 mL conical flask and incubated in Dulbecco's Modified Eagle's Medium (DMEM) medium containing 0.25% trypsin, 1% glucose, 0.75 mg mL^{-1} collagenase, proteinase inhibitor cocktail (1:100), 5 μg mL^{-1} deoxyribonuclease I and 100 IU penicillium-streptomycin for 1 h at 37°C under stirring gently. These tissues were then washed with fresh DMEM medium and filtered through 70 and 40 μm nylon filters (BD Falcon, Bedford, MA, USA) to discard debris. The filtrate containing approximately 2×10^6 testicular cells per mL was washed with BPS buffer, fixed in ethanol (70%) for 1 h, centrifuged at 800× *g* for 6 min and resuspended in PBS. Ribonuclease A (100 μg mL^{-1}) was added to these cells and they were then stained with propidium iodide (PI; 50 μg mL^{-1}) for 30 min at 37°C. The stained cells were filtered through a 40 μm nylon mesh and sorted by flowcytometry (FACScan; Becton Dickinson System, San Jose, CA, USA). With a FACS Vantage flowcytometry and cell sorter interfaced to a Macintosh operating system equipped with the CELL QUEST software (Becton-Dickinson, USA), the PI fluorescence of these testicular cells was monitored upon emission wavelength at 610 nm when excited wavelength was at 488 nm. Four parameters were measured for each cell: forward scatter (FSC-H), side scatter (SSC-H) (data not shown) (Malkov *et al.*, 1998), total fluorescence emitted from the cell (FL2-A) and duration of emitted fluorescence from the cell (FL2-W), which correlates with nuclear diameters. Triplicate specimens were prepared per animal group, and at least 10 000 events were calculated for each sample. The relative proportions of testicular cells were estimated from the area under the peak curve in the DNA histogram.

Analysis of cytochrome c release from mitochondria to cytosol
Cytochrome *c* resides chiefly in the mitochondrial intermembrane space in resting cells. Stimuli that induce release of cytochrome *c* from mitochondria to cytosol trigger a cascade of cell signalling and lead to apoptosis (Green and Reed, 1998). The activity of this mitochondrion-dependent apoptotic process could be estimated from the ratio of the cytosolic to the mitochondrial cytochrome *c* fractions (Kasahara *et al.*, 2002). To investigate whether Dox and EGb modulate the distribution of this apoptotic factor, mitochondrial and cytosolic fractions of cellular proteins were isolated as reported before (Ogawa *et al.*, 2002; Yeh *et al.*, 2007). In short, fresh testicular tissues were homogenized in ice-cold 1X Cytosol Extraction Buffer Mix (BioVision, Mountain View, CA, USA) containing DTT and protease inhibitors. Ten minutes later, these tissues were homogenized by an ice-cold glass Dounce tissue grinder on ice for 15 times, and were then centrifuged at 700× *g* for 10 min at 4°C to remove the pellets. The supernatants were further centrifuged at 10 000× *g* for 30 min at 4°C to separate the cytosolic (in the supernatant) and the mitochondrial (in the pellets) fractions of the cytoplasmic proteins. The mitochondrial fractions were finally resuspended with Mitochondrial Extraction Buffer Mix (BioVision, Mountain View, CA, USA) containing DTT and protease inhibitors, vortexed for 10 s to obtain the mitochondrial fraction and stored at –80°C till use. To determine the relative abundance of cytochrome *c* in the compartments of mitochondria and cytosol, 50 μg of proteins from mitochondrial and cytosolic extracts were subjected to 15% SDS-PAGE followed by immunoblotting analysis.

Determination of caspase-3 and caspase-8 activities
Caspase-3 and caspase-8 activities in the testicular tissues were measured with the colorimetric CaspACE assay system (Promega, Madison, WI, USA). Briefly, samples were lysed in 50 μL Cell Lysis Buffer and centrifuged at 10 000× *g* for 20 min. The supernatants were collected and the protein concentrations were determined using Bradford Protein Assay. The protein lysates (50 μg) were added to the caspase assay buffer containing 20 mmol·L^{-1} of caspase-3 substrate Ac-DEVD-pNA or caspase-8 substrate Ac-IETD-pNA and incubated at 37°C for 4 h. Reaction mixtures without testis extract were used as negative controls. Production of the yellow colour released from the substrate upon cleavage by caspase-3 or caspase-8 was monitored with spectrofluorometry (Hitachi U-1500) at 405 nm, and the extent of yellow colour detected was proportional to the caspase-3 and caspase-8 activities present in the samples.

Statistical analysis
All experiments were repeated at least three times, and one representative from these experiments with similar results is shown. The quantitative data of continuous variables were expressed as mean ± SEM Statistical significance was tested by Student's *t*-test or ANOVA with *post hoc* analysis when appropriate. A P value < 0.05 was considered statistically significant.

Chemicals and drugs
Doxorubicin was purchased from Pfizer Italia S.R.L. (Milano, Italy). EGb (equivalent to 0.84 mg mL^{-1} *Ginkgo* flavonoglycosides, calculated as quercetin, kaempferol and isorhametin) was obtained from Dr Willmar Schwabe GmbHz Co. (Karlsruhe, Germany). Anti-cytochrome *c* and anti-p53 antibodies were from Lab Vision Corp. (Fremont, CA, USA). Anti-prohibitin antibody (mitochondrial marker), anti-Bid antibody and anti-Apaf-1 antibody were respectively from Abcam (Cambridge, MA, USA) and Cell Signaling Technology (Beverly, MA, USA). Anti-TNFR-1 and anti-TRAIL-1 antibodies were from Upstate Biotechnology (Lake Placid, NY, USA). HRP-conjugated secondary antibodies to mouse, rabbit and goat immunoglobulins were purchased from Zymed Laboratories (San Franscisco, CA, USA). PI was from Molecular Probe (Eugene, OR, USA). All other antibodies were from Santa Cruz Biotechnology (Santa Cruz, CA, USA), and chemicals from Sigma (St. Louis, MO, USA) or Fisher Scientific (Fairlawn, NJ, USA).

Table 1 Effects of doxorubicin (Dox) and EGb 761 on body and testicular weights, sperm cell counts, and spermatogenic structures

n	*Cont*	*Dox*	*EGb*	*EGbDox*
	10	*10*	*10*	*10*
Body weight (BW)				
Baseline (g)	312 ± 14	313 ± 8	307 ± 3	313 ± 5
Final (g)	355 ± 16	264 ± 8§	341 ± 4	329 ± 8**
Gain (final vs. baseline, %)	14 ± 2	–15 ± 1§	11 ± 1	5 ± 1§**
Testicular weight*				
Absolute (g)	3.51 ± 0.12	3.02 ± 0.07‡	3.44 ± 0.13	3.34 ± 0.07#
Relative (vs. final BW, %)	0.99 ± 0.05	1.16 ± 0.04†	1.01 ± 0.05	1.01 ± 0.01#
Epididymal sperm counts ($\times 10^6$)*	7.43 ± 0.58	3.45 ± 0.31§	7.77 ± 0.28	6.61 ± 0.30**
Seminiferous tubules				
Number	634 ± 55	344 ± 73†	777 ± 19†	531 ± 16¶
Diameter (μm)	304 ± 5	252 ± 8§	295 ± 3	271 ± 3†¶

*Sum of both testes.
†$P < 0.05$, ‡$P < 0.01$ and §$P < 0.001$ versus Cont group.
¶$P < 0.05$, #$P < 0.01$ and **$P < 0.001$ versus Dox group.
EGb, *Ginkgo biloba* extract 761.

Results

Effects of Dox and EGb on body growth, testicular weight and spermatogenic structures

During the entire study period Dox-treated animals (Dox) gained much less weight than the controls (Cont) (Table 1). In contrast, those pretreated with EGb (EGbDox) were largely spared from this growth-retarding effect of Dox (EGbDox vs. Dox, $P = 0.0001$), although their body weight was still less than the control (EGbDox vs. Cont, $P = 0.001$). These results suggested that EGb could partially antagonize the negative effect of Dox on body growth. A similar antagonism of Dox and protection, by EGb pretreatment (EGbDox), on the growth of testes could be deduced from the significant between-group difference in testicular weight (Dox vs. Cont, $P = 0.003$; EGbDox vs. Dox, $P = 0.01$; Table 1). The relative testicular weight (ratio of absolute testicular weight to final body weight) was higher in the Dox group rats as compared with the control and the EGb-pretreated animals (Table 1), indicating that within a short period (7 days) of exposure, the growth suppression of Dox and EGb was more marked on whole body weight, than on testicular weight.

Microscopically, Dox disrupted rat spermatogenic structures, causing swelling of seminiferous tubules and depletion of spermatids (Fig. 1, Dox), whereas EGb pretreatment significantly alleviated these abnormalities (Fig. 1, EGbDox). Quantitatively, the amount of epididymal sperms, number of testicular tubules and diameter of seminiferous tubules were notably decreased by Dox (Table 1) and, again, pretreatment with EGb largely counteracted these unfavourable actions of Dox and preserved the integrity of spermatogenic structures.

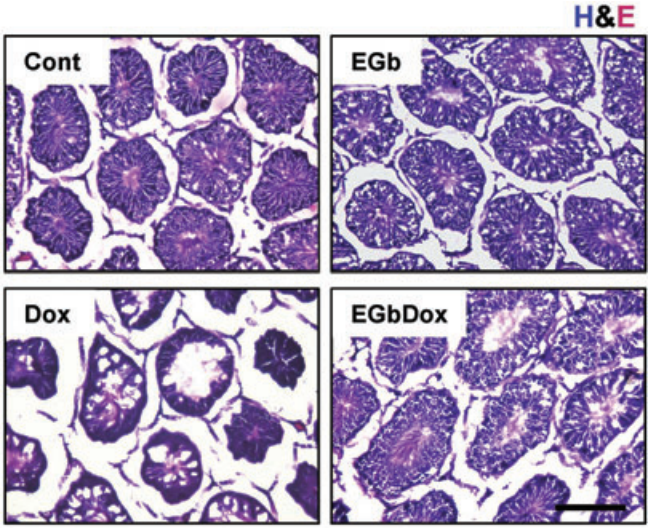

Figure 1 Representative illustrations of histological morphology of rat testes. Cross sections of testes were stained with hematoxylin and eosin (H and E). Testes from control (Cont) and *Ginkgo biloba* extract 761 (EGb) groups of rats exhibit typical features of seminiferous epithelium, while those from doxorubicin (Dox) group animals display impaired spermatogenesis and miniature seminiferous tubules. In rats pretreated with EGb (EGbDox), testes could be protected from these Dox-induced abnormalities and show nearly normal histological morphology in testicular sections. Scale bar = 200 μm.

EGb ameliorated Dox-inflicted oxidative stress by attenuating reactive oxygen species generation and preventing antioxidant enzyme deactivation

The quantity of reactive oxygen species and the activity of antioxidant enzymes reflect the state of oxidative stress within a tissue (Singal and Iliskovic, 1998). Dox-treated testes (Dox) contained significantly higher levels of MDA, a product of lipid-peroxidation (vs. control, $P = 0.003$, Fig. 2A), and lower activity of SOD (vs. control, $P = 0.006$, Fig. 2B), GPx (vs. control, $P = 0.0002$ Fig. 2C) and GSH (vs. control, $P = 0.0003$ Fig. 2D), indicating the potent pro-oxidative actions of Dox on testicular tissues. EGb pretreatment (EGbDox) neutralized these abnormalities both in MDA (EGbDox vs. Dox, $P = 0.028$, Fig. 2A) and in GSH levels ($P = 0.002$; Fig. 2D). EGb also normalized anti-oxidant enzyme activity ($P = 0.015$ for SOD, $P = 0.007$ for GPx; Fig. 2B,C), showing the effect of EGb against Dox-induced oxidative stress in testes.

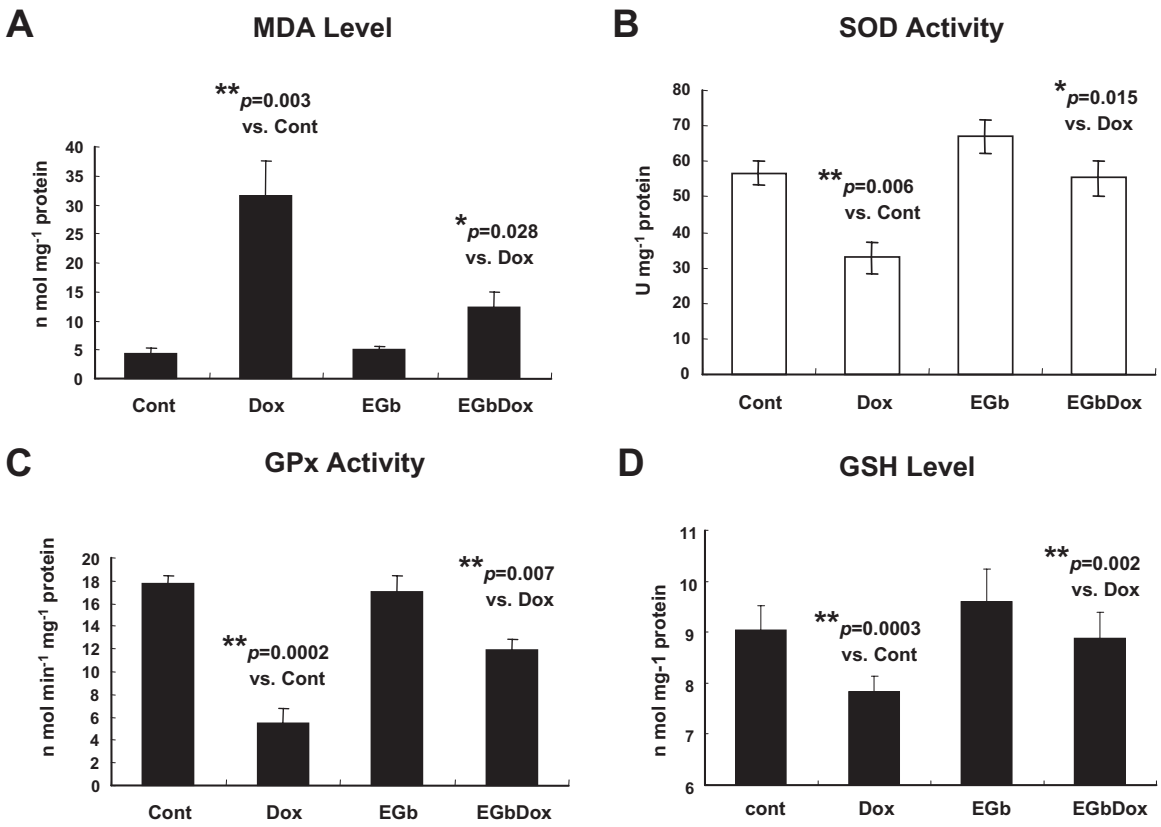

Figure 2 Attenuation of doxorubicin (Dox)-induced oxidative stress by EGb in rat testicular tissue. (A) MDA level. Dox significantly increased the content of this free radical surrogate in testicular tissue, compared with control (Cont), while EGb pretreatment (EGbDox) significantly alleviated its generation. (B) Total SOD activity. The activity of this intrinsic antioxidant enzyme was markedly depressed in the Dox group (Dox) as compared with the Cont (Cont), whereas EGb pre-treatment significantly prevented this outcome. (C) and (D) Total GPx activity and GSH activity. The effects of Dox and EGb on the activity of these two antioxidant enzymes are similar. Values are presented as mean ± SEM ($n = 3$ in each group). EGb, *Ginkgo biloba* extract 761; GPx, glutathione peroxidase; MDA, malondialdehyde; SOD, superoxide dismutase.

Testicular tissues are protected from oxidative stress by both extrinsic (i.e. serum) and intrinsic antioxidant enzymes (Sikka, 2004). To further clarify whether Dox and EGb exert differential effects on these antioxidant systems, serum and testicular tissues from all groups of rats were collected for comparative analysis. In serum, Dox significantly decreased the concentrations of both SOD1 (vs. controls, $P = 0.0007$, Fig. 3A) and SOD2 (vs. controls, $P = 0.002$, Fig. 3B), while EGb pretreatment effectively sustained activities of both isoforms (vs. Dox, $P = 0.01$ for SOD1 and $P = 0.004$ for SOD2). In testicular tissues, however, SOD1 was much more predominately expressed at basal state and was the only SOD member that was subject to Dox downregulation and EGb preservation (Fig. 3C,D). Thus the tissue-specific SOD enzyme in testes and the circulating SODs were affected by Dox and EGb, both locally and systemically.

EGb suppressed pro-apoptotic effects of Dox through inhibiting p53 targeted protein expressions, cytochrome c release, caspase-3 cleavage and caspase-3 activity in testes

Doxorubicin is a well-known pro-apoptotic agent. To evaluate whether EGb protected testicular cells through inhibiting Dox-induced cell apoptosis, testicular tissues and testicular cells were assessed by TUNEL and flow cytometric assays (Fig. 4). After 7 days of treatment, testicular tissues exposed to Dox contained more TUNEL-positive staining (Fig. 4A,B, Dox vs. Cont, $P = 0.0002$) in contrast to those pretreated with EGb (EGbDox vs. Dox, $P = 0.017$), indicating the pro-apoptotic effects of Dox and anti-apoptotic effects of EGb in testes.

Flow cytometric analysis of PI-labeled testicular cells provides reliable quantification of differentiating testicular cell subpopulations based on their DNA staining (Hacker-Klom *et al.*, 1986). To clearly determine the effect of Dox and EGb on the process of spermatogenesis and sperm cell apoptosis, suspended testicular cells of rats were subjected to flow cytometric analysis. The first window harvested from flow cytometry (Fig. 4C, left columns) describes FL2-A plotted against FL2-W and displays dot plot areas. The second window (Fig. 4D, left columns) demonstrates the main histogram peaks that represent the number of cells at each fluorescent level (FL2-A). Seven distinct populations (R1 to 7) could be identified (Malkov *et al.*, 1998): cells shown as R1 and R2 contained 4d DNA and consisted of primary spermatocytes; cells shown as R3 and R4 contained 2d DNA and consisted of major somatic cells, spermatogonia, preleptotene spermatocytes and secondary spermatocytes; cells shown as R5–7 consisted of spermatids and mature spermatozoa. The histogram of apoptotic cells will shift leftward to main spermatid populations and appear as a sub-haploid

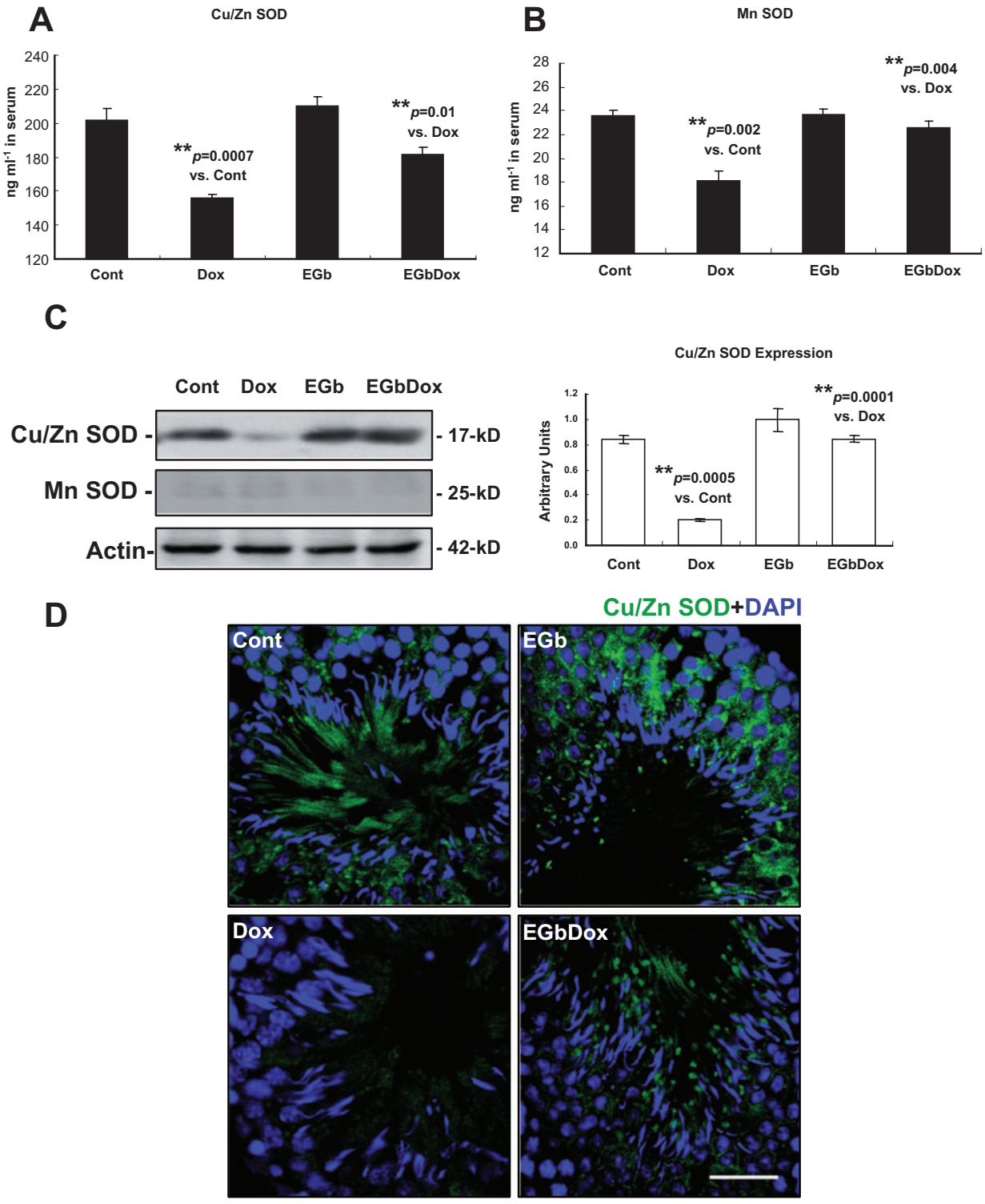

Figure 3 Effects of doxorubicin (Dox) and EGb on circulating and testicular SOD expression. (A) and (B) ELISA study. Levels of both Cu/Zn and Mn SOD were significantly depressed in serum of Dox-treated rats (Dox) as compared with the control (Cont), while EGb pre-treatment (EGbDox) prevented this effect of Dox. Values are obtained from three independent experiments and expressed as mean ± SEM (C) Immunoblotting study. Abundance of Cu/Zn SOD in testicular extracts of Dox-treated rats (Dox) was markedly diminished, except where these animals had been pretreated with EGb (EGbDox). Representative sets of data are shown from three independent immunoblotting analyses. Summary data from densitometry of Western blots of Cu/Zn SOD expression are also shown and presented as mean ± SEM ($n = 3$ in each group). Only low levels of Mn SOD were present in all groups of animals. (D) Cellular distribution of Cu/Zn SOD protein in the testes from all groups. Cu/Zn SOD was predominantly present in spermatids near the seminiferous lumen. The Cu/Zn SOD signal intensity was markedly lower in the Dox group compared with control, but was only slightly reduced in EGbDox group. Green fluorescence indicates the locations of Cu/Zn SOD, and blue colour represents testicular sections counterstained with DAPI. Scale bar = 20 μm. DAPI, 4′,6′ diamidino-2-phenylindole; EGb, *Ginkgo biloba* extract 761; SOD, superoxide dismutase.

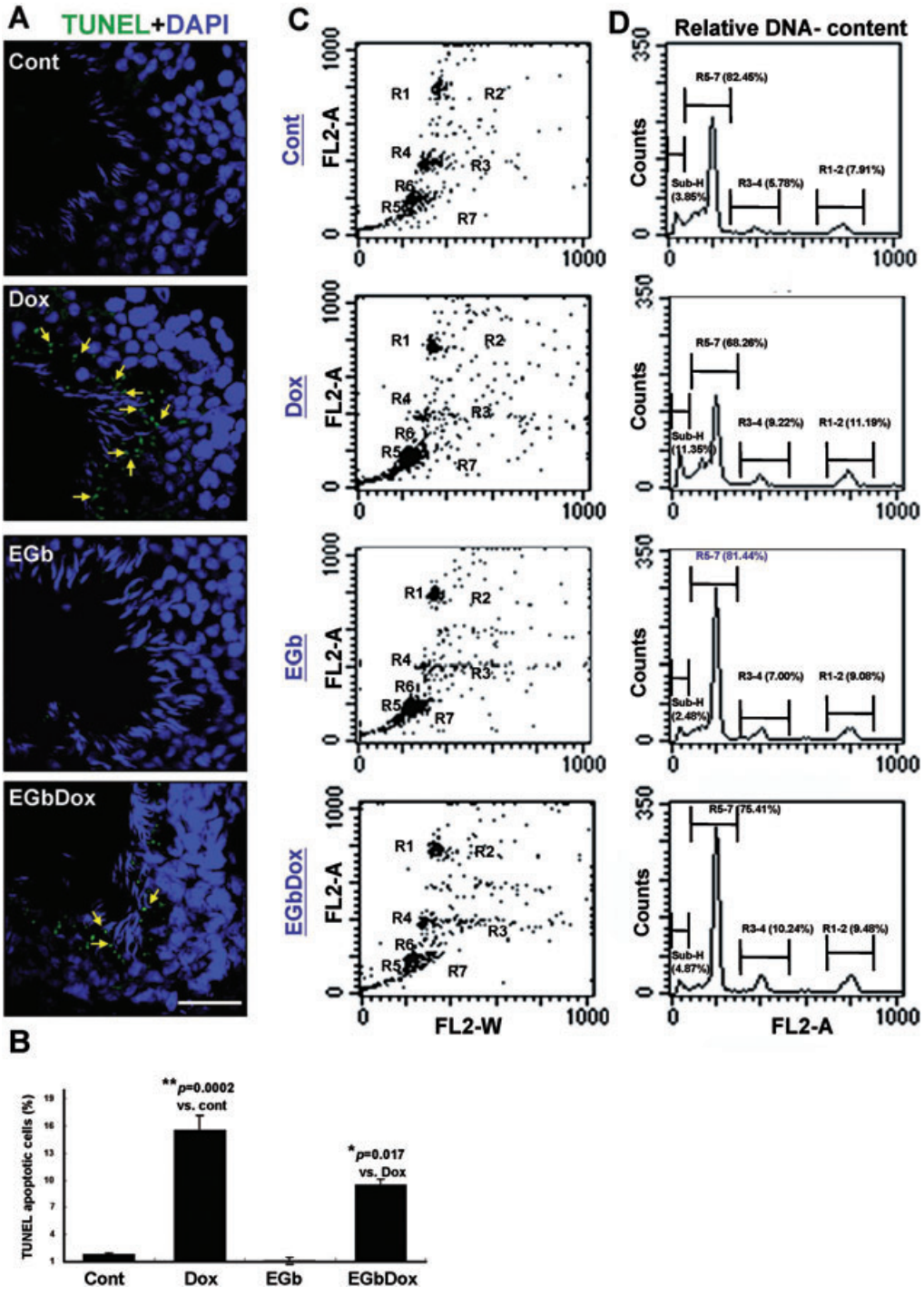

Figure 4 Effects of doxorubicin (Dox) and EGb on testicular cell apoptosis and spermatogenesis. (A) TUNEL assay. Testicular sections from Dox-treated rats (Dox) show significantly more positive TUNEL-positive (i.e. apoptotic) cells (green signals, arrows), compared with the control (Cont), while EGb pretreatment (EGbDox) largely neutralized this apoptotic action of Dox on testis. Blue color represents testicular cells counterstained with DAPI. Scale bar = 10 μm. (B) Quantitative analysis of TUNEL results. Dox significantly increases TUNEL apoptotic index (ratio of TUNEL-positive to DAPI-stained cells) in testicular tissue, whereas EGb pretreatment inhibited this increase in the apoptotic index. (C) Flow cytometric analysis of suspended PI-stained testicular cells. Testicular cells are distributed according to fluorescence intensity (FL2-A channel) in arbitrary units presented on logarithmic scale and width of the emitted fluorescence (FL2-W channel) displayed on the horizontal axes. Locations of gated groups are marked by their group numbers (R1 to 7). (D) The histograms represent the numbers of cells (counts) at each fluorescence level (FL2-A channel) and the proportion of each subgroup (R1–2, R3–4 or R5–7, sub-haploid) to total cell counts (%). Proportion of haploid germ cells (R5–7 peak), or mature spermatozoa, is significantly decreased in Dox-treated rats (Dox) as compared with the Cont group (68.3% vs. 82.5%, $P = 0.003$), while EGb pre-treatment (EGbDox) preserved this population at 75.4% (vs. Dox, $P = 0.02$), illustrating the deleterious effect of Dox and the counteracting action of EGb on spermatogenesis. Proportion of apoptotic cells represented by the sub-haploid (sub-H) peak increases to 11.4% in Dox group as compared with the control (3.9%), but could be suppressed to 4.9% by EGb pretreatment (EGbDox). Values are obtained from three independent experiments and presented as mean ± SEM. DAPI, 4′,6′ diamidino-2-phenylindole; EGb, *Ginkgo biloba* extract 761; TUNEL, terminal deoxynucleotidyl transferase nick-end labelling.

(sub-H) peak, reflecting cell shrinkage due to chromosome condensation (Sherwood and Schimke, 1995; Selva *et al.*, 2000). Our data showed that the haploid cell population (mature spermatozoa, R5–7) was reduced to 68.3% by Dox as compared with control (82.5%) (Dox vs. Cont, $P = 0.03$), but was largely restored to 75.4% by EGb pretreatment (EGbDox vs. Dox, $P = 0.02$), indicating the deleterious effect of Dox and the protective action of EGb on spermatozoa production. On the other hand, the sub-haploid population (apoptotic cells) was increased to 11.4% by Dox in comparison to the control (3.9%), while pre-treatement with EGb maintained this population at 4.9%, confirming the pro-apoptotic effect of Dox and the anti-apoptotic effects of EGb on testicular cells.

To determine the apoptotic and anti-apoptotic signalling mechanisms responsible for the effects of Dox and the EGb in testes, the expressions of cytosolic pro-apoptotic proteins (Bax, Bad) as well as the anti-apoptotic factors (Bcl-2, Bcl-xL) were examined by immunoblotting and immunofluroscence analyses. In Dox-treated testes, the abundance of Bax and Bad was significantly upregulated, whereas that of Bcl-2 and Bcl-xL was downregulated (Fig. 5A,B), resulting in a decrease of the Bcl-2/Bax ratio (an index of cell resistance to apoptosis) to 0.4 as compared with 0.8 in the control ($P = 0.047$) (Fig. 5A). This apoptosis-resistance index could be largely protected by EGb up to a value of 0.6 (vs. Dox, $P = 0.019$), implying the involvement of Bcl-2 family proteins in the anti-apoptotic action of EGb.

To further delineate the signalling pathway of Dox-induced apoptosis, cellular p53, Apaf-1 and mitochondrion-related apoptotic factors were examined. The expressions of p53 and Apaf-1 were markedly upregulated in testicular tissues (Fig. 5C), along with marked elevation of cytosolic cytochrome *c* content from 33% to 57% of the total cellular abundance (Dox vs. Cont, $P = 0.001$) (Fig. 6A, right panel). Besides, Dox significantly increased caspase-3 activation as reflected by the production of cleaved caspase-3 (Fig. 6A) and increase of caspase-3 activity (Dox vs. Cont, $P = 0.001$) (Fig. 6B), depicting the role of the p53-mediated, mitochondrion-dependent (or intrinsic) apoptotic pathway in Dox testicular toxicity. Dox-elicited upregulation of p53, induction of Apaf-1, depolarization of mitochondrial potential, release of cytochrome *c* from mitochondria to cytosol (EGbDox vs. Dox, $P = 0.004$) and activation of caspase-3 (EGbDox vs. Dox, $P = 0.028$) could all be neutralized by EGb pretreatment, indicating the potent counteracting action of EGb against Dox at nearly all cellular levels of this pathway.

To determine whether the extrinsic apoptotic pathway was also involved in the action of Dox and EGb on testicular cells, crucial factors mediating the extrinsic apoptotic pathway, including death receptor Fas, tissue necrosis factor receptor 1 (TNFR-1), tumour necrosis factor-related apoptosis-inducing ligand-1 (TRAIL-1), caspase 8 and Bid were examined. Immunoblotting studies showed that the cellular level of Fas was not influenced by either Dox or EGb (Fig. 6D), suggesting that Fas was not involved in the apoptotic action of Dox and the protective effect of EGb in testes. On the other hand, the TNFR/TRAIL-mediated apoptotic signalling pathway all the way from expression of TNFR-1 and TRAIL-I, activation of caspase-8 (Fig. 6C) to cleavage of Bid to t-Bid (Fig. 6D) was evoked by Dox but was not suppressed by EGb pretreatment, suggesting this apoptotic signalling pathway could possibly be involved in the pathogenic action of Dox, but not in the protective effect of EGb on testes.

Discussion and conclusions

Male germ cells are known to be one of the tissues vulnerable to Dox toxicity (Suter *et al.*, 1997; Hou *et al.*, 2005). The potentially infertility-causing complication renders protection of testicular tissue a critical issue whenever Dox is employed for anti-neoplastic chemotherapy. Our previous study has shown that Dox impaired mouse testicular structure through inflicting oxidative stress and inducing cell apoptosis (Yeh *et al.*, 2007). The present study further provides evidence that pre-treatment with EGb, a standardized extract from *Ginkgo biloba* leaves, could effectively alleviate Dox-induced toxicity to testes. These findings raise the possibility that EGb may be a an adjuvant therapy, potentially protecting the testes from oxidative and apoptotic actions related to Dox, and might help, ultimately, to prevent this devastating adverse effect of Dox in clinical practice.

Untoward effects of Dox on rat spermatogenesis

Doxorubicin exerts its cytotoxic action through intercalating into the DNA backbone of neoplastic cells and interfering with cell division. The adverse effects of this anti-tumour agent, in contrast, result chiefly from its inherent tendency to generate free radicals and suppress antioxidant enzymes in various tissues (Atessahin *et al.*, 2006). The current study confirmed that lipid peroxidation, a downstream chain reaction initiated by free radicals, was activated by Dox as reflected by the increased level of lipoperoxidation product, MDA, in testes, demonstrating the extraordinary sensitivity of this tissue to free radical injury by this exogenous, pro-oxidative agent, Dox. This phenomenon could be at least partially attributable to the structure of the male germ cell membrane, which is rich in polyunsaturated fatty acids and is thereby particularly prone to lipid peroxidation (Lenzi *et al.*, 2002). The high levels of DNA synthesis and cellular proliferation in these cells may also play a role in the susceptibility of spermatozoa to damage by free radicals (Bauche *et al.*, 1994; Sikka, 2004). Moreover, our findings also demonstrated that at least two crucial endogenous antioxidant enzymes (SOD and GPx), responsible for scavenging superoxide radicals were markedly suppressed by Dox, which might cause excessive consumption, reduced production, or chemical deactivation of these enzymes (Doroshow, 1983; Mohan *et al.*, 2006). Furthermore, testicular tissue is inherently deficient in a potent component of the SOD family (SOD2). These features together contribute to the sensitivity of testicular tissue to Dox oxidative injury (Kasahara *et al.*, 2002; Sikka, 2004) and, accordingly, suggest anti-oxidants as one of the therapeutic options to protect the testes from Dox injury.

Apoptosis plays a causative role to the development of Dox toxicity in various tissues (Shinoda *et al.*, 1999; Nakamura *et al.*, 2000). The mechanism responsible for this process of programmed cell death remains still controversial, but direct

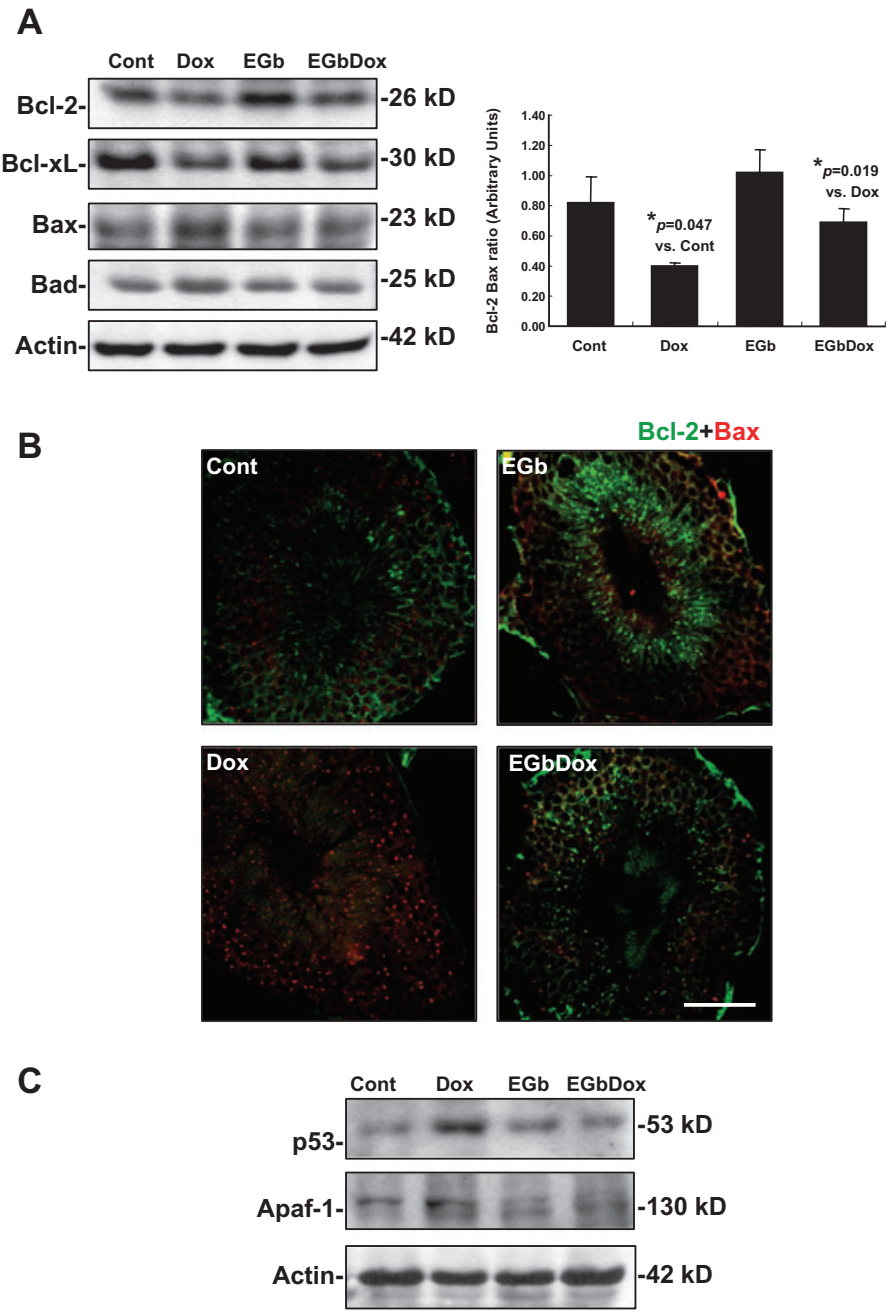

Figure 5 Modulation of Bcl-2 family proteins, p53 and Apaf-1 by doxorubicin (Dox) and EGb in rat testicular tissues. (A) On the left, imunoblotting study of Bcl-2 family proteins. Dox substantially upregulates the crucial pro-apoptotic factors (Bax, Bad) and downregulates the key anti-apoptotic proteins (Bcl-2, Bcl-xL) of the Bcl-2 family in testicular tissues. EGb pretreatment (EGbDox) partly reversed these apoptosis-inducing reactions. Representative sets of data from three independent experiments are shown. On the right, summary data of the ratio of Bcl-2 to Bax from densitometry are presented as mean ± SEM ($n = 3$ in each group). (B) Immunofluroscence analyses of the cellular distribution of Bcl-2 (green fluorescence) and Bax (red signals) proteins in testicular sections. Increased expression of Bax and decreased expression of Bcl-2 could be clearly observed in testicular sections from Dox-treated (Dox) rats and EGb pre-treatment (EGbDox) prevented much of this Dox-induced pro-apoptotic phenomenon. Scale bar = 10 μm. (C) Immunoblotting study of p53 and Apaf-1. Dox significantly stimulated p53 and Apaf-1 protein expressions in testicular tissue, while EGb pretreatment (EGbDox) markedly reduced upregulation of these factors. EGb, *Ginkgo biloba* extract 761.

mitochondrial injury by free radicals (Doroshow, 1983) or indirect mitochondrial depolarization by pro-apoptotic Bcl-2 family proteins (Jurgensmeier *et al.*, 1998) have been proposed as critical components of the processh. Our study further demonstrated that two important intrinsic apoptotic pathway effectors, p53 and Apaf-1, were responsive to Dox stimulation in testes, as reported by Long *et al.* (1997) in heart tissue. As p53 responds to both DNA damage and oxidative stress to trigger downstream apoptotic signalling, the mechanism for Dox apoptosis seems to originate both from the pharmacological consequences of DNA injury and from oxidative stress. The involvement of the upstream apoptotic pathway mediator p53, the pro-apoptotic Bcl-2 family protein Bax/Bad, the apoptotic stimulator Apaf-1 and the

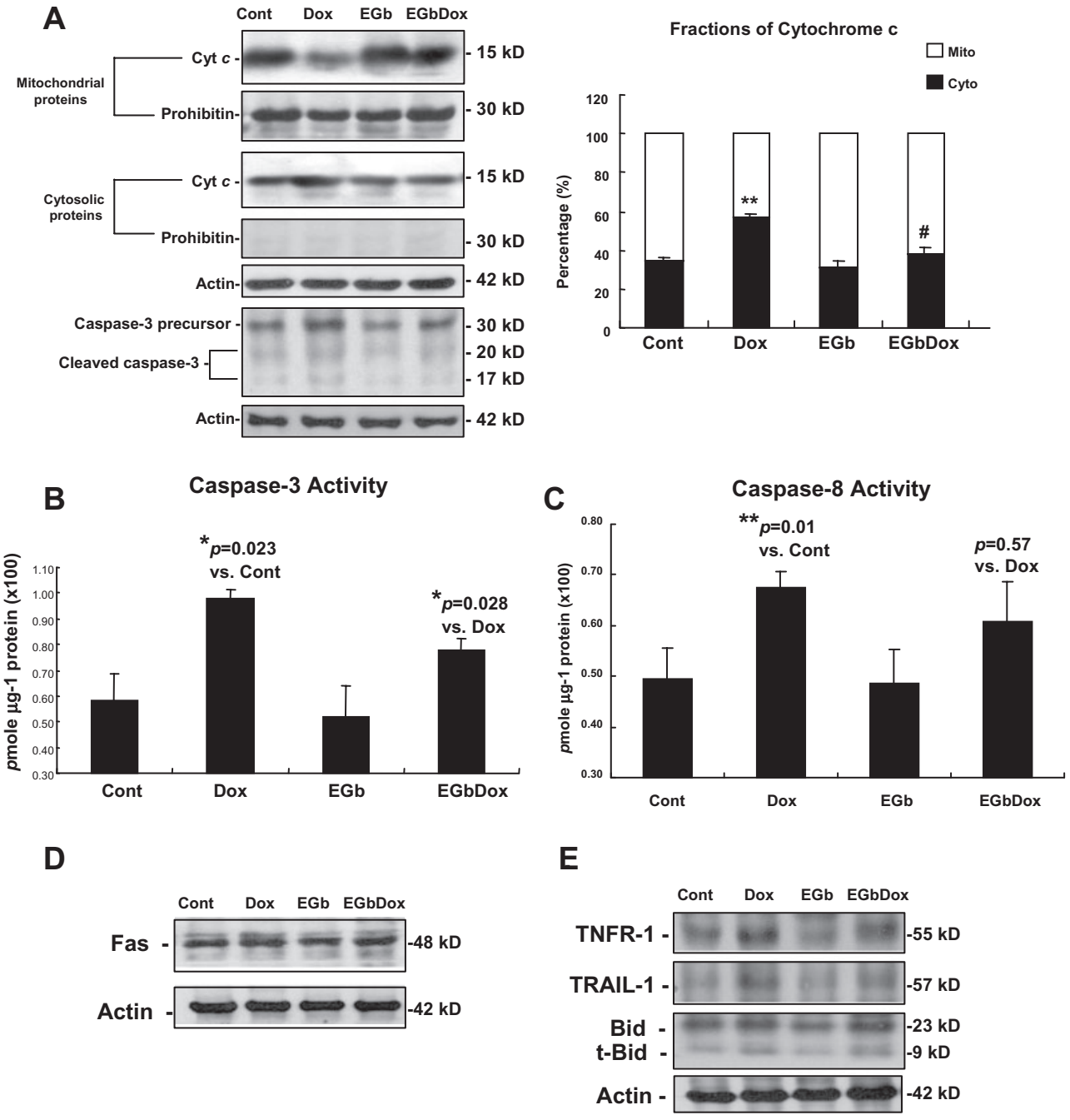

Figure 6 Effects of doxorubicin (Dox) and EGb on release of cytochrome *c*, activity of caspase-3/-8, and abundance of extrinsic apoptotic pathway mediators Fas, TRAIL-1, Bid and TNFR in rat testicular tissue. (A) Immunoblotting study of mitochondrial and cytosolic cytochrome *c*. The ample presence of a specific mitochondrial marker, prohibitin, in the mitochondrial extracts (lane 2) and absence of this marker in the cytosolic fractions (lane 4) demonstrates the relative purity of both protein fractions. The abundance of cytochrome *c* was strikingly increased in the cytosol (lane 1) and decreased in the mitochondria (lane 3) in response to Dox treatment (Dox), indicating the triggering effect of Dox on cytochrome *c* release from mitochondria to cytosol. This shuttling of cytochrome *c* could be prevented by EGb pretreatment (EGbDox). On the right, summary data on the cellular distribution of cytochrome *c* in Dox-treated rats (Dox) and with EGb pretreatment (EGbDox) are presented (Cont vs. Dox, $*P = 0.0004$; EGbDox vs. Dox, $\#P = 0.004$; means ± SEM, $n = 4$). Cyto, cytosolic fraction of cytochrome *c*; Mito, mitochondrial fraction of cytochrome *c*.

In the last panel in (A), the level of cleaved caspase-3, a product and marker of capase-3 activation, was markedly higher in Dox-treated (Dox) than EGb-pretreated (EGbDox) testicular tissue (lane 4). (B) Caspase-3 activity. Dox increased the activity of caspase-3 by 1.68-fold, whereas EGb pretreatment (EGbDox) inhibited this increase. Values are mean ± SEM from three independent experiments. (C) Caspase-8 activity. Dox treatment (Dox) significantly elevated caspase-8 activity in testicular tissue, while EGb pretreatment (EGbDox) did not antagonize this effect of Dox. (D) Immunoblotting of Fas. Expression of this extrinsic apoptotic pathway initiator was not influenced by either Dox or EGb, indicating that this death receptor does not play a role in the apoptotic effect of Dox or the protective action of EGb in testes. (E) Immunoblotting of Bid, TRAIL-I and TNFR-1. All these factors as well as the product of Bid activation, t-Bid, were upregulated in the testicular tissue of Dox-treated (Dox) rats and were not suppressed by EGb pretreatment (EGbDox), suggesting that these extrinsic apoptotic pathway mediators may be involved in the apoptotic effect of Dox but not in the protective action of EGb against Dox toxicity. EGb, *Ginkgo biloba* extract 761.

mitochondrion-dependent downstream apoptotic effectors in the toxic effect of Dox strongly suggest that the p53-initiated, Apaf-1-fascilitated, mitochondrion-dependent apoptotic signalling, i.e. the intrinsic apoptotic pathway, was responsible for Dox apoptotic toxicity. Delineation of the signalling pathway from the upstream p53, Apaf-1 and Bcl-2 family proteins to downstream mitochondrion-dependent caspase cascade system could help effective intervention in this process by blockade at any signalling level.

Protective effects of EGb on Dox-induced testicular toxicity

Ginkgo biloba leaves have been used for thousands of years as a traditional herbal medicine, yet the beneficial effect of this plant was only recently demonstrated on disorders of the CNS such as Alzheimer's disease, cerebrovascular occlusion, i.e. ischemic cerebral stroke and peripheral arterial insufficiency, as in intermittent claudication, all of which could be attributed to its well-known anti-platelet and anti-cytokine effects (De Smet, 2002). This extract, EGb, may enhance penile blood flow to improve male impotence through modulating some vasoactive substances, including nitric oxide, prostaglandin and platelet activating factor, but whether this compound of multiple constituents exerts net beneficial effect on testicular cells remains undetermined (Al-Yahya *et al*., 2006). This *in vivo* study for the first time illustrated the capability of EGb in attenuating testicular lipid peroxidation and protecting circulating and testis-specific antioxidant enzyme activities in rats exposed to Dox, illustrating the dual anti-oxidative actions of EGb against a potent free radical-producing chemotherapeutic agent. This antioxidant effect of EGb has been linked to certain compounds in its main constituents, flavonoids and terpenoids, which can scavenge free radicals and reduce level of reactive oxygen species (De Smet, 2002; DeFeudis *et al*., 2003; Smith and Luo, 2004), as has been shown in this study to effectively abolish the lipid peroxidation elicited by Dox. The findings that the stimulatory effects of EGb on both circulating and testis-specific antioxidant enzyme activities were only present in testes after exposure to Dox suggest that EGb protected these defensive antioxidant enzymes by counteracting the deactivating action of Dox, rather than by directly stimulating expression of these enzymes. This result differs from a previous study where EGb increased the transcription of antioxidant enzymes (mitochondrial SOD, haem oxygenase 1) in different tissue and cells (Gohil and Packer, 2002), suggesting tissue-to-tissue variation in the effects of EGb. In the especially vulnerable testicular tissue, the dual antioxidant actions of EGb together contribute synergistically to the marked inhibition of Dox-induced oxidative stress.

The current study also elucidated the effective suppression of apoptosis and rescue of germ cells by EGb in testes exposed to Dox. This anti-apoptotic effect of EGb has been reported elsewhere, but the mechanism responsible for this process was not defined. Among the various known pathways responsible for apoptosis, EGb has been shown to moderate apoptosis induced by beta-amyloid in neuronal cells, through influencing mitochondrial membrane potentials, regulating Bcl-2 family members and repressing caspase-3 activity (Bastianetto *et al*., 2000; Luo *et al*., 2002; Smith and Luo, 2004). Our findings identified similar mechanisms, namely the mitochondrion-dependent pathway, through which EGb antagonized Dox-induced apoptosis of haploid spermatids. Additionally, among the diverse triggering signals converging on the mitochondria, this study specifically recognized that p53 and Apaf-1, two Dox-triggered effectors upstream of the intrinsic apoptotic pathway, were neutralized by EGb, along with the downstream factors all the way through the mitochondrial-dependent apoptotic pathway. These results clearly depict the potent anti-apoptotic effect of EGb against Dox at nearly all levels in the intrinsic apoptotic pathway. Importantly, as p53 is a crucial endogenous tumour suppressor, indiscriminate repression of this factor carries the risk of tumorigenesis. However, given that EGb inhibits p53 expression only when the testis is exposed to the stress of Dox, and EGb itself could suppress tumour growth through antioxidant, anti-angiogenic and gene-regulating actions (DeFeudis *et al*., 2003), it is less likely that treatment with EGb would induce carcinogenesis. Finally, the anti-tumour effect of Dox is also not likely to be influenced by adjuvant EGb, as the anti-neoplastic action of Dox is achieved mainly through DNA-intercalation rather than through oxidative or p53-mediated apoptotic action. This interpretation is supported by two previous studies demonstrating that EGb did not reduce the anti-tumour effect of Dox in mice bearing H22 hepatoma (one minor Chinese study announced in 1999) or gastric carcinoma (Agha *et al*., 2001).

Whether Dox-induced apoptosis involves the other apoptosis-related cell signalling, or extrinsic apoptotic, pathway remains controversial (Li *et al*., 2007; Reeve *et al*., 2007). Our finding that cellular levels of Fas were not altered by Dox in testicular tissue, as also noted in heart (Liu *et al*., 2008), has minimized possible roles of Fas-mediated apoptotic pathway in pathogenesis of Dox testicular toxicity. In contrast, as the TNF family-induced extrinsic apoptotic signalling, including expression of TNFR-1 and TRAIL-1, activation of caspase 8 and cleavage of Bid to t-Bid (Yamada *et al*., 1999; Li *et al*., 1998), could be upregulated by Dox but not suppressed by EGb, it can be deduced that Dox may induce testicular cell apoptosis at least partially through activating TNFR/TRAIL-mediated extrinsic pathway, which cannot be effectively antagonized by EGb. Further study is needed to determine, in more detail, the role of this apoptotic pathway in the deleterious effect of Dox and the protective effect of EGb in testes.

In conclusion, this *in vivo* study provides evidence that Dox adversely damages testicular tissue and significantly reduces sperm production through increasing oxidative stress and inducing apoptosis, while EGb pre-treatment effectively attenuated these oxidative and apoptotic actions of Dox in testes. As Dox-based chemotherapy is still indispensable for treatment of various cancers but drug-induced infertility is often unavoidable, our results open a window for prevention of this devastating testicular complication by adjuvant administration of the versatile herbal medicine EGb, which might hopefully be the answer to this serious testicular toxicity induced by Dox.

Acknowledgements

The authors are grateful to Mei-Chun Liu for her assistance with flow cytometric and confocal microscopic assays. The

authors also express thanks to Chung-Che Tsai, Chien-Sheng Hsu and Hsiao-Han Huang for their technical assistance. This study was supported in part by Yen-Tjing-Ling Medical Foundation (CI-96 to C. T. Ting) and Taichung Veteran General Hospital Research Grants (TCVGH-963108C to T. J. Liu; TCVGH-966303C to H. C. Lai).

Conflict of interest

None declared.

References

Agha AM, El-Fattah AA, Al-Zuhair HH, Al-Rikabi AC (2001). Chemopreventive effect of Ginkgo biloba extract against benzo(a)pyrene-induced forestomach carcinogenesis in mice: amelioration of doxorubicin cardiotoxicity. *J Exp Clin Cancer Res* **20**: 39–50.

Al-Yahya AA, Al-Majed AA, Al-Bekairi AM, Al-Shabanah OA, Qureshi S (2006). Studies on the reproductive, cytological and biochemical toxicity of Ginkgo Biloba in Swiss albino mice. *J Ethnopharmacol* **107**: 222–228.

Atessahin A, Turk G, Karahan I, Yolmaz S, Ceribasi AO, Bulmus O (2006). Lycopene prevents adriamycin-induced testicular toxicity in rats. *Fertil Steril* **85** (Suppl 1): 1216–1222.

Bastianetto S, Ramassamy C, Dore S, Christen Y, Poirier J, Quirion R (2000). The Ginkgo biloba extract (EGb 761) protects hippocampal neurons against cell death induced by beta-amyloid. *Eur J Neurosci* **12**: 1882–1890.

Bauche F, Fouchard MH, Jegou B (1994). Antioxidant system in rat testicular cells. *FEBS Lett* **349**: 392–396.

Bradford MM (1976). A rapid and sensitive method for the quantitation of microgram quantities of protein utilizing the principle of protein-dye binding. *Anal Biochem* **72**: 248–254.

Da Cunha MF, Meistrich ML, Ried HL, Gordon LA, Watchmaker G, Wyrobek AJ (1983). Active sperm production after cancer chemotherapy with doxorubicin. *J Urol* **130**: 927–930.

De Smet PA (2002). Herbal remedies. *N Engl J Med* **347**: 2046–2056.

Defeudis FV, Papadopoulos V, Drieu K (2003). Ginkgo biloba extracts and cancer: a research area in its infancy. *Fundam Clin Pharmacol* **17**: 405–417.

Doroshow JH (1983). Effect of anthracycline antibiotics on oxygen radical formation in rat heart. *Cancer Res* **43**: 460–472.

Gohil K (2002). Genomic responses to herbal extracts: lessons from in vitro and in vivo studies with an extract of Ginkgo biloba. *Biochem Pharmacol* **64**: 913–917.

Gohil K, Packer L (2002). Global gene expression analysis identifies cell and tissue specific actions of Ginkgo biloba extract, EGb 761. *Cell Mol Biol (Noisy-le-grand)* **48**: 625–631.

Green DR, Reed JC (1998). Mitochondria and apoptosis. *Science* **281**: 1309–1312.

Hacker-Klom UB, Meistrich ML, Gohde W (1986). Effect of doxorubicin and 4′-epi-doxorubicin on mouse spermatogenesis. *Mutat Res* **160**: 39–46.

Hou M, Chrysis D, Nurmio M, Parvinen M, Eksborg S, Soder O *et al*. (2005). Doxorubicin induces apoptosis in germ line stem cells in the immature rat testis and amifostine cannot protect against this cytotoxicity. *Cancer Res* **65**: 9999–10005.

Howell SJ, Shalet SM (2005). Spermatogenesis after cancer treatment: damage and recovery. *J Natl Cancer Inst Monogr* **2005**: 12–17.

Jahnukainen K, Jahnukainen T, Salmi TT, Svechnikov K, Eksborg S, Soder O (2001). Amifostine protects against early but not late toxic effects of doxorubicin in infant rats. *Cancer Res* **61**: 6423–6427.

Jurgensmeier JM, Xie Z, Deveraux Q, Ellerby L, Bredesen D, Reed JC (1998). Bax directly induces release of cytochrome c from isolated mitochondria. *Proc Natl Acad Sci USA* **95**: 4997–5002.

Kasahara E, Sato EF, Miyoshi M, Konaka R, Hiramoto K, Sasaki J *et al*. (2002). Role of oxidative stress in germ cell apoptosis induced by di(2-ethylhexyl)phthalate. *Biochem J* **365**: 849–856.

Koksal T, Erdogru T, Toptas B, Gulkesen KH, Usta M, Baykal A *et al*. (2002). Effect of experimental varicocele in rats on testicular oxidative stress status. *Andrologia* **34**: 242–247.

Lenzi A, Gandini L, Lombardo F, Picardo M, Maresca V, Panfili E *et al*. (2002). Polyunsaturated fatty acids of germ cell membranes, glutathione and blutathione-dependent enzyme-PHGPx: from basic to clinic. *Contraception* **65**: 301–304.

Li H, Zhu H, Xu CJ, Yuan J (1998). Cleavage of BID by caspase 8 mediates the mitochondrial damage in the Fas pathway of apoptosis. *Cell* **94**: 491–501.

Li S, Zhou Y, Dong Y, Ip C (2007). Doxorubicin and selenium cooperatively induce fas signaling in the absence of Fas/Fas ligand interaction. *Anticancer Res* **27**: 3075–3082.

Liu TJ, Yeh YC, Ting CT, Lee WL, Wang LC, Lee HW *et al*. (2008). Ginkgo biloba extract 761 reduces doxorubicin-induced apoptotic damage in rat hearts and neonatal cardiomyocytes. *Cardiovasc Res* **80**: 227–235.

Logani S, Chen MC, Tran T, Le T, Raffa RB (2000). Actions of Ginkgo Biloba related to potential utility for the treatment of conditions involving cerebral hypoxia. *Life Sci* **67**: 1389–1396.

Long X, Boluyt MO, Hipolito ML, Lundberg MS, Zheng JS, O'Neill L *et al*. (1997). p53 and the hypoxia-induced apoptosis of cultured neonatal rat cardiac myocytes. *J Clin Invest* **99**: 2635–2643.

Lu G, Wu Y, Mak YT, Wal SM, Feng ZT, Rudd JA *et al*. (2006). Molecular evidence of the neuroprotective effect of Ginkgo biloba (EGb761) using bax/bcl-2 ratio after brain ischemia in senescence-accelerated mice, strain prone-8. *Brain Res* **1090**: 23–28.

Luo Y, Smith JV, Paramasivam V, Burdick A, Curry KJ, Buford JP *et al*. (2002). Inhibition of amyloid-beta aggregation and caspase-3 activation by the Ginkgo biloba extract EGb761. *Proc Natl Acad Sci USA* **99**: 12197–12202.

Malkov M, Fisher Y, Don J (1998). Developmental schedule of the postnatal rat testis determined by flow cytometry. *Biol Reprod* **59**: 84–92.

Mohan IK, Kumar KV, Naidu MU, Khan M, Sundaram C (2006). Protective effect of CardiPro against doxorubicin-induced cardiotoxicity in mice. *Phytomedicine* **13**: 222–229.

Nakamura T, Ueda Y, Juan Y, Katsuda S, Takahashi H, Koh E (2000). Fas-mediated apoptosis in adriamycin-induced cardiomyopathy in rats: in vivo study. *Circulation* **102**: 572–578.

Ogawa Y, Nishioka A, Kobayashi T, Kariya S, Hamasato S, Saibara T *et al*. (2002). Mitochondrial cytochrome c release in radiation-induced apoptosis of human peripheral T cells. *Int J Mol Med* **10**: 263–268.

Quinn R (2005). Comparing rat's to human's age: how old is my rat in people years? *Nutrition* **21**: 775–777.

Reeve JL, Szegezdi E, Logue SE, Chonghaile TN, O'Brien T, Ritter T *et al*. (2007). Distinct mechanisms of cardiomyocyte apoptosis induced by doxorubicin and hypoxia converge on mitochondria and are inhibited by Bcl-xL. *J Cell Mol Med* **11**: 509–520.

Selva DM, Tirado OM, Toran N, Suarez-Quian CA, Reventos J, Munell F (2000). Meiotic arrest and germ cell apoptosis in androgen-binding protein transgenic mice. *Endocrinology* **141**: 1168–1177.

Shen J, Wang J, Zhao B, Hou J, Gao T, Xin W (1998). Effects of EGb 761 on nitric oxide and oxygen free radicals, myocardial damage and arrhythmia in ischemia-reperfusion injury in vivo. *Biochim Biophys Acta* **1406**: 228–236.

Sherwood SW, Schimke RT (1995). Cell cycle analysis of apoptosis using flow cytometry. In: Schwartz LM, Osborne BA (eds). *Methods in Cell Biology*, Vol. 46. Academic Press: San Diego, pp. 77–97.

Shinoda K, Mitsumori K, Yasuhara K, Uneyama C, Onodera H, Hirose

M *et al*. (1999). Doxorubicin induces male germ cell apoptosis in rats. *Arch Toxicol* **73**: 274–281.

Sikka SC (2004). Role of oxidative stress and antioxidants in andrology and assisted reproductive technology. *J Androl* **25**: 5–18.

Singal PK, Iliskovic N (1998). Doxorubicin-induced cardiomyopathy. *N Engl J Med* **339**: 900–905.

Smith JV, Luo Y (2004). Studies on molecular mechanisms of Ginkgo biloba extract. *Appl Microbiol Biotechnol* **64**: 465–472.

Suter L, Bobadilla M, Koch E, Bechter R (1997). Flow cytometric evaluation of the effects of doxorubicin on rat spermatogenesis. *Reprod Toxicol* **11**: 521–531.

Tan C, Etcubanas E, Wollner N, Rosen G, Gilladoga A, Showel J *et al*. (1973). Adriamycin – an antitumor antibiotic in the treatment of neoplastic diseases. *Cancer* **32**: 9–17.

Timioglu O, Kutsal S, Ozkur M, Uluoglu O, Aricioglu A, Cevik C *et al*. (1999). The effect of EGb 761 on the doxorubicin cardiomyopathy. *Res Commun Mol Pathol Pharmacol* **106**: 181–192.

Yamada H, Tada-Oikawa S, Uchida A, Kawanishi S (1999). TRAIL causes cleavage of bid by caspase-8 and loss of mitochondrial membrane potential resulting in apoptosis in BJAB cells. *Biochem Biophys Res Commun* **265**: 130–133.

Yeh YC, Lai HC, Ting CT, Lee WL, Wang LC, Wang KY *et al*. (2007). Protection by doxycycline against doxorubicin-induced oxidative stress and apoptosis in mouse testes. *Biochem Pharmacol* **74**: 969–980.

Yoon CY, Hong CM, Cho YY, Chung YH, Min HK, Yun YW *et al*. (2003). Flow cytometric assessment of ethylene glycol monoethyl ether on spermatogenesis in rats. *J Vet Med Sci* **65**: 207–212.